Tropical Plants

ARTICLE

Open Access

https://doi.org/10.48130/tp-0026-0032

Tropical Plants **2026**, 5: e032

*EgGRF*1-*EgGIF*3 co-expression enhances transformation and screening efficiency in *Agrobacterium*-mediated transformation of oil palm

Authors

Can Luo, Tingting Zhang, Fuheng Yuan, Chao Ouyang, Jixin Zou*, Dongdong Li*

Correspondence

zourich@163.com (Zou J);
lidd@hainanu.edu.cn (Li D)

In Brief

This study identifies EgGRF1 and EgGIF3 as positive regulators of oil palm callus differentiation. Co-expression of EgGRF1-EgGIF3 significantly improves *Agrobacterium*-mediated transformation screening efficiency (5.32%) and differentiation rate (56.39%) in oil palm embryogenic tissues, providing an optimized protocol and candidate genes for functional studies in this recalcitrant tropical crop.

Graphical abstract

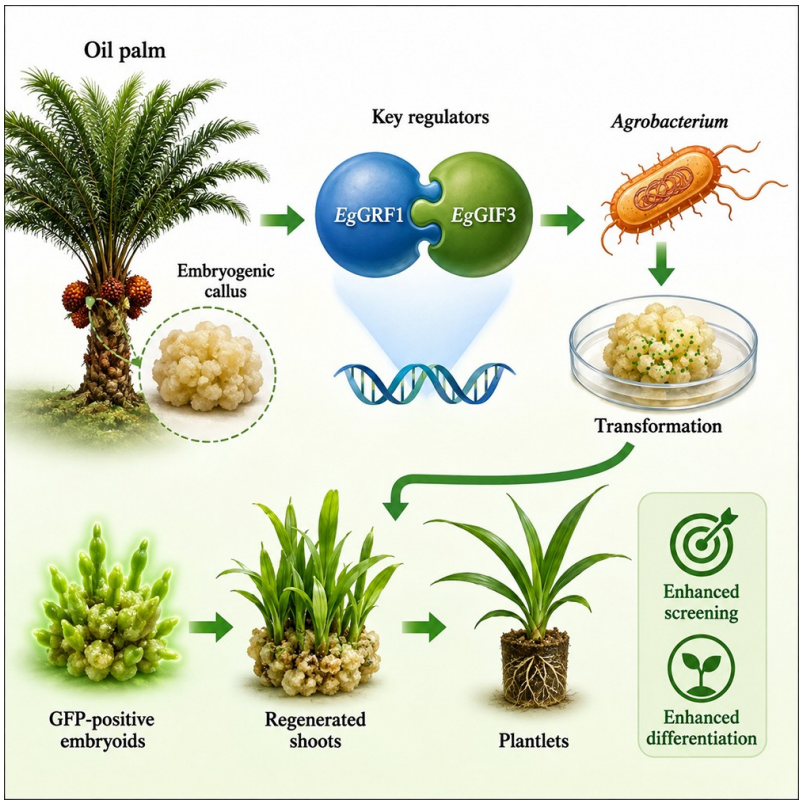

Highlights

- Genome-wide identification reveals 14 *EgGRF* and 4 *EgGIF* genes in oil palm.
- *EgGRF*1 and *EgGRF*7 physically interact with *EgGIF*3.
- Optimized *Agrobacterium*-mediated transformation achieves 3.58% screening efficiency.
- *EgGRF*1-*EgGIF*3 co-expression improves screening efficiency (5.32%) and differentiation (56.39%).

Citation: Luo C, Zhang T, Yuan F, Ouyang C, Zou J, et al. 2026. *EgGRF*1-*EgGIF*3 co-expression enhances transformation and screening efficiency in *Agrobacterium*-mediated transformation of oil palm. *Tropical Plants* 5: e032 https://doi.org/10.48130/tp-0026-0032

© The Author(s)

Tropical Plants

ARTICLE

Open Access

https://doi.org/10.48130/tp-0026-0032

Tropical Plants **2026**, 5: e032

*EgGRF*1-*EgGIF*3 co-expression enhances transformation and screening efficiency in *Agrobacterium*-mediated transformation of oil palm

Can Luo[1], Tingting Zhang[1], Fuheng Yuan[1], Chao Ouyang[2], Jixin Zou[2*] and Dongdong Li[1*]

[1] *National Key Laboratory for Tropical Crop Breeding, College of Tropical Agriculture and Forestry, Hainan University, Sanya 572025, China*
[2] *Coconut Research Institute of Chinese Academy of Tropical Agricultural Sciences (CATAS), Wenchang 571339, China*
* Correspondence: zourich@163.com (Zou J); lidd@hainanu.edu.cn (Li D)

Abstract

Oil palm (*Elaeis guineensis* Jacq.) is a tropical woody oil crop with high economic value, but its low genetic transformation efficiency hinders molecular breeding. Growth-regulating factors (GRFs) and GRF-interacting factors (GIFs) play key roles in plant regeneration, yet their functions in oil palm remain unexplored. Here, we identified 14 *EgGRF* and 4 *EgGIF* genes via genome-wide analysis. Transcriptome and RT-qPCR showed that *EgGRF*1, *EgGRF*7, and *EgGIF*3 were significantly upregulated in regenerable tissues, and dual-luciferase assays confirmed protein interactions between *EgGRF*1/*EgGRF*7 and *EgGIF*3. We then optimized *Agrobacterium*-mediated transformation parameters, achieving a screening efficiency of 3.58% under optimal conditions (OD_{600} = 0.5, infection for 40 min, 200 μmol/L acetosyringone, 60 h co-cultivation). Functional evaluation revealed that *EgGRF*1-*EgGIF*3 co-expression significantly increased both screening efficiency (5.32% ± 0.34%) and differentiation rate (56.39%), outperforming single-gene transformations. *EgGRF*1 alone also markedly improved differentiation (49.46%). Collectively, these results demonstrate that *EgGRF*1 is a key positive regulator of oil palm callus differentiation, and its synergistic expression with *EgGIF*3 further enhances screening efficiency and differentiation capacity at the embryogenic stage, providing an optimized protocol and candidate genes for oil palm genetic improvement.

Keywords: Oil palm, GRF-GIF co-expression, Callus regeneration, Screening efficiency, Growth-regulating factor

Citation: Luo C, Zhang T, Yuan F, Ouyang C, Zou J, et al. 2026. *EgGRF*1-*EgGIF*3 co-expression enhances transformation and screening efficiency in *Agrobacterium*-mediated transformation of oil palm. *Tropical Plants* 5: e032 https://doi.org/10.48130/tp-0026-0032

Introduction

Oil palm (*Elaeis guineensis* Jacq.) is a perennial tropical woody oil crop belonging to the Arecaceae family. It is the most efficient oil-producing crop worldwide, with palm oil accounting for approximately one-third of global vegetable oil production[1]. The fruit mesocarp and kernel yield palm oil and palm kernel oil, which are widely used in food processing, industrial manufacturing, and biofuel production[2]. Despite its economic importance, oil palm breeding remains challenging due to its long life cycle (10–15 years from seed to maturity), large plant size, and complex genetic background. Conventional hybridization has made limited progress in developing high-yielding and stress-tolerant varieties, particularly for cultivation in marginal environments such as the northern tropical regions of China[3]. Therefore, the development of efficient genetic transformation systems is urgently needed to accelerate molecular breeding and gene function studies in oil palm.

Tissue culture has been established as a powerful tool for clonal propagation of oil palm, enabling large-scale production of uniform planting materials[4]. Embryogenic callus derived from various explants, including immature zygotic embryos, leaves, and inflorescences, has been successfully used for plant regeneration[5,6]. However, the regeneration process is time-consuming, often taking 12–18 months from callus induction to plantlet acclimatization, and the efficiency remains highly genotype-dependent[7]. To overcome these limitations, genetic transformation approaches have been explored to introduce beneficial genes that promote cell proliferation, somatic embryogenesis, and shoot regeneration. Among various transformation methods, *Agrobacterium*-mediated transformation offers several advantages, including low transgene copy number, stable integration, and cost-effectiveness[8]. Although oil palm is a monocot and not a natural host for *Agrobacterium*, successful transformations have been reported using embryogenic callus as explants, with transformation efficiencies typically below 1%[9,10]. Optimization of key parameters such as bacterial concentration, infection duration, acetosyringone (AS) concentration, and co-cultivation time is therefore critical for improving transformation efficiency in recalcitrant species like oil palm[11].

Growth-regulating factors (GRFs) are plant-specific transcription factors that play essential roles in regulating cell proliferation, organ growth, and development. The GRF protein family is characterized by two highly conserved domains at the N-terminus: the QLQ domain (Gln-Leu-Gln), which mediates interaction with GRF-interacting factors (GIFs), and the WRC domain (Trp-Arg-Cys), which is responsible for DNA binding and nuclear localization[12,13]. Since the first identification of OsGRF1 in rice, GRF family members have been characterized in numerous plant species, including Arabidopsis[12], soybean[14], sorghum[15], and birch[16]. GIFs are transcriptional co-activators that lack DNA-binding activity but contain an SNH (SSXT) domain that enables interaction with GRFs and recruitment of chromatin remodeling complexes[17,18]. The GRF-GIF complex has been shown to promote cell proliferation and organ expansion by activating downstream target genes involved in cell cycle regulation[19]. Overexpression of GRFs has been reported to increase leaf size in Arabidopsis[12], Chinese cabbage[20], and lettuce[21], while GRF-GIF co-expression has been demonstrated to enhance regeneration efficiency in multiple crops. Notably, Debernardi et al.[22] showed that a chimeric GRF-GIF fusion protein significantly improved

transformation efficiency and regeneration capacity in wheat, rice, and citrus, providing a promising strategy for recalcitrant plant species.

Despite the established roles of GRF and GIF genes in plant growth and regeneration, their functions in oil palm have not been systematically characterized. In this study, we performed genome-wide identification and characterization of the *EgGRF* and *EgGIF* gene families in oil palm. Based on transcriptome and qPCR analyses, we identified candidate genes that are highly expressed in regenerable callus. We then optimized key parameters of *Agrobacterium*-mediated transformation using oil palm embryogenic callus as explants. Finally, we evaluated the effects of single and co-expression of *EgGRF*1, *EgGRF7*, and *EgGIF*3 on transformation screening efficiency and callus differentiation rate. The results demonstrate that *EgGRF*1-*EgGIF*3 co-expression significantly enhances transformation screening efficiency and differentiation capacity at the callus/embryogenic stage, providing an optimized protocol and valuable gene resources for functional studies in oil palm.

Materials and methods

Plant materials

Embryogenic calli of oil palm (*Elaeis guineensis* Jacq.) were provided by the Coconut Research Institute, Chinese Academy of Tropical Agricultural Sciences (CATAS). Calli were subcultured monthly on maintenance medium (MS basal medium with appropriate hormones, pH 5.8) at 25 ± 2 °C in the dark. *Nicotiana benthamiana* plants used for dual-luciferase assays were grown at 25 °C under a 16-h light/8-h dark photoperiod.

Identification and bioinformatic analysis of *EgGRF* and *EgGIF* genes

The GRF and GIF gene families in oil palm were identified through BLASTP searches (E-value ≤ 1×10^{-40}) using query sequences from *Arabidopsis thaliana*, *Oryza sativa*, and *Zea mays*. Conserved domains (QLQ and WRC for GRFs; SSXT for GIFs) were validated using Pfam and SMART. Phylogenetic trees were constructed using MEGA 7.0 with the neighbor-joining method (1,000 bootstrap replicates). Conserved motifs were analyzed using MEME, gene structures using GSDS 2.0, and promoter *cis*-elements (2,000 bp upstream) using PlantCARE. Chromosomal locations and synteny were analyzed with MCScanX and visualized using TBtools.

Transcriptome sequencing and RT-qPCR

Total RNA was extracted from robust regenerable callus (RC) and poorly growing browned callus (PC) using the RNAprep Pure Plant Kit (Tiangen, Beijing). RNA-seq libraries were prepared and sequenced on an Illumina platform. Clean reads were aligned to the oil palm reference genome using HISAT2, and expression levels were quantified as FPKM. For RT-qPCR, first-strand cDNA was synthesized using the TransScript Kit (TransGen, Beijing). qPCR was performed using 2× SYBR Green Master Mix (Takara) on an ABI 7500 FAST system with three biological replicates. The oil palm Actin gene served as the internal control, and relative expression was calculated using the $2^{-\Delta\Delta CT}$ method.

Dual-Luciferase complementation imaging (LCI) assay

The coding sequences of *EgGRF*1 and *EgGRF7* were cloned into the pCAMBIA1300-nLUC vector, and *EgGIF*3 was cloned into pCAMBIA1300-cLUC. Constructs were transformed into *Agrobacterium* strain GV3101 (pSoup). Co-infiltrations into *N. benthamiana* leaves were performed as follows: (++) nLUC-GRF + cLUC-GIF; (+) nLUC-empty + cLUC-GIF; (−) nLUC-empty + cLUC-empty; (−+) nLUC-GRF + cLUC-empty. After 48 h, luciferase activity was detected using a plant living imaging system (Tanon, China).

Vector construction and *Agrobacterium* transformation

The coding sequences of *EgGRF*1, *EgGRF7*, and *EgGIF*3 were amplified from oil palm callus cDNA. For single-gene overexpression, amplicons were cloned into the pNC-Cam1304-MCS35S vector using the NimbleCloning (NC) kit (Nimble, China). For co-expression constructs, *EgGRF*1 (without a stop codon) and *EgGIF*3 were fused by overlap extension PCR; the same strategy was used for *EgGRF7*-*EgGIF*3. All constructs were confirmed by Sanger sequencing and transformed into *Agrobacterium* strain EHA105.

For transformation optimization, embryogenic calli were pre-cultured on Murashige and Skoog (MS0) medium for 3–4 d. *Agrobacterium* suspensions were prepared at OD_{600} values of 0.4–0.8, and calli were infected for 20–50 min. Acetosyringone (AS) concentrations of 50–250 μmol/L were tested. After infection, calli were co-cultivated at 20 °C for 36–84 h, then washed with timentin (500 mg/L) and placed on selection medium containing 60 mg/L hygromycin B. Subculturing was performed every 3 weeks.

Screening efficiency and differentiation rate

Green fluorescent protein (GFP) fluorescence was observed under a LUYOR-3415 excitation light source. Screening efficiency was calculated as (Number of GFP-positive embryoids after 3–4 rounds of selection/Total number of infected calli) × 100. GFP-positive embryoids were identified based on stable fluorescence under a LUYOR-3415 excitation light source. Differentiation rate was calculated as (Number of GFP-positive regenerated shoots derived from embryoids/Total number of GFP-positive embryoids) × 100.

PCR confirmation

Genomic DNA was extracted from hygromycin-resistant embryoids using the Plant Genomic DNA Kit (Tiangen, Beijing, China). Embryoids were the primary tissue type used for PCR analysis due to their abundance after selection. Where available, DNA was also extracted from embryogenic calli and regenerated shoots for additional verification, though these materials were limited in quantity. The presence of the hygromycin resistance gene (Hyg) was detected by PCR using specific primers (Hyg-F and Hyg-R). For co-expression constructs, gene-specific primers spanning the fusion junction were used to confirm the presence of the intact fusion gene in transgenic materials at different developmental stages.

Statistical analysis

All experiments were performed with three independent biological replicates. Data were expressed as mean ± standard deviation (SD). Statistical analyses were performed using GraphPad Prism 10 software. Comparisons among multiple groups were conducted using one-way ANOVA followed by Tukey's multiple comparison test. Differences with $p < 0.05$ were considered statistically significant, and $p < 0.01$ (**) or $p < 0.0001$ (****) were considered highly significant.

https://doi.org/10.48130/tp-0026-0032

Results

Identification and characterization of *EgGRF* and *EgGIF* gene families

A total of 14 *EgGRF* and 4 *EgGIF* genes were identified in the oil palm genome through genome-wide analysis. The *EgGRF* proteins ranged from 260 to 605 amino acids in length, with molecular weights from 27.62 to 65.30 kDa and theoretical pI values from 5.88 to 9.28 (Supplementary Table S1). All *EgGRF* proteins exhibited instability indices above 40 and negative GRAVY values, suggesting that most *EgGRF* proteins may be unstable under *in vitro* conditions. The four *EgGIF* proteins ranged from 191 to 222 amino acids, with molecular weights from 20.15 to 23.85 kDa and pI values below 7.

Phylogenetic analysis of GRF proteins from oil palm, Arabidopsis, rice, and maize revealed that all GRF members could be classified into three subfamilies (I, II, and III) (Fig. 1a). Subfamily II contained the largest number of members (23), while subfamily I contained the fewest (8). The 14 *EgGRF* members were distributed across all three subfamilies. Conserved motif analysis showed that all *EgGRF* proteins contained the characteristic QLQ and WRC domains (motif1 and motif2), while some members also possessed an additional motif3 (Fig. 1b). All four *EgGIF* proteins contained the conserved SSXT domain (Fig. 1c). Promoter *cis*-element analysis revealed that both *EgGRF* and *EgGIF* genes harbor multiple elements related to hormone responses (ABRE, TGA-element, P-box), light responses (G-box, I-box, ACE), and stress responses (LTR, TC-rich repeats) (Fig. 1d). Chromosomal localization and synteny analysis indicated that *EgGRF* and *EgGIF* genes are distributed across 16 chromosomes, with several segmental duplication events observed (Supplementary Fig. S1).

Expression patterns of *EgGRF*s and *EgGIF*s in different callus types

To identify candidate GRF and GIF genes potentially involved in callus proliferation and regeneration, transcriptome sequencing was performed on RC and poorly growing, browned callus (PC) (Fig. 2a). Differential expression analysis revealed that several *EgGRF* genes, including *EgGRF*1, *EgGRF*2, *EgGRF*3, and *EgGRF*7, were significantly upregulated in RC compared to PC (Fig. 2b). Among the *EgGIF* genes, *EgGIF*2 and *EgGIF*3 showed significantly higher expression in RC.

RT-qPCR was further performed to validate the transcriptome results. Consistent with the RNA-seq data, *EgGRF*1 and *EgGRF*7 exhibited significantly higher expression levels in RC than in PC, with *EgGRF*1 showing the most pronounced difference ($p < 0.0001$)

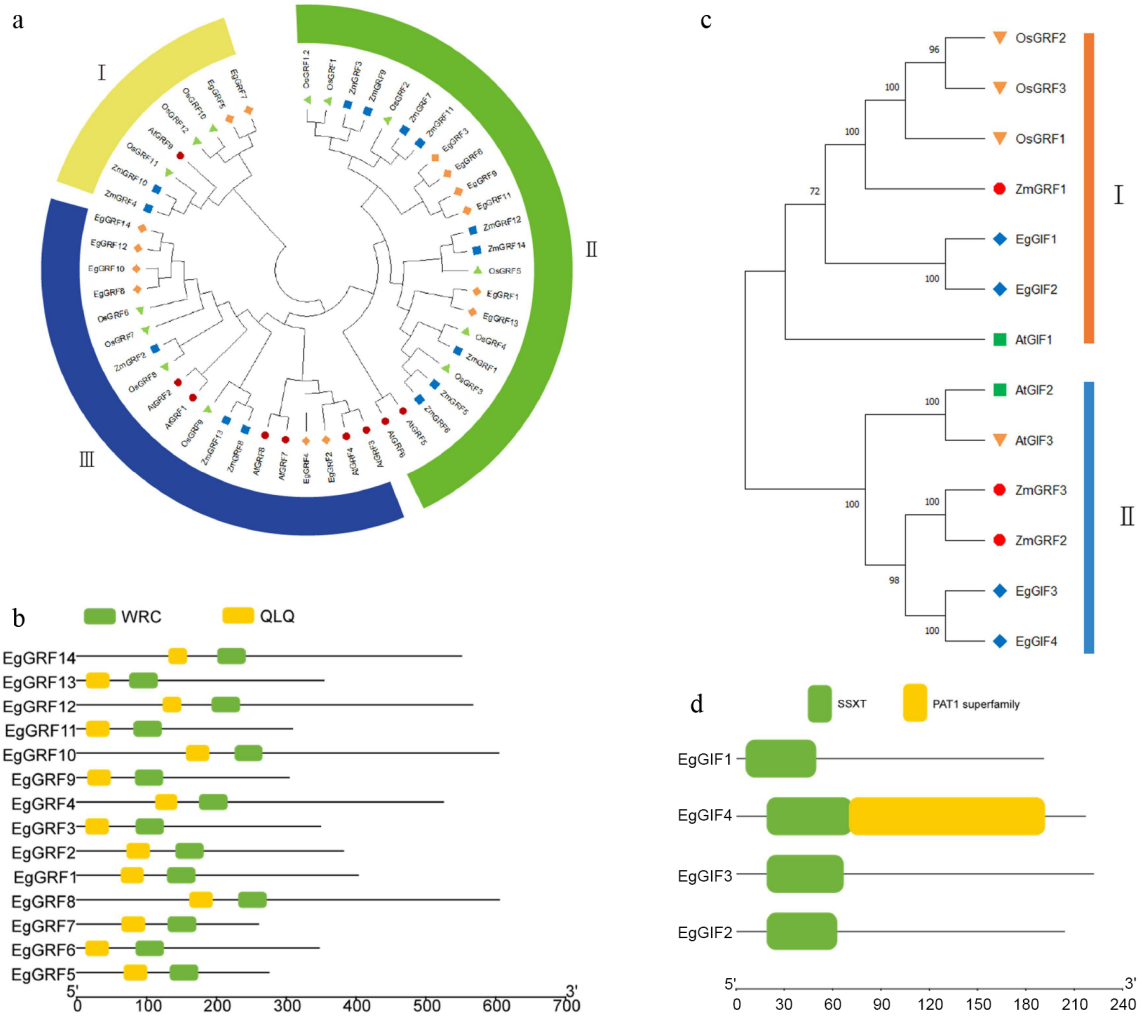

Fig. 1 Phylogenetic relationships and conserved domains of *EgGRF* and *EgGIF* genes in oil palm. (a) Phylogenetic tree of the GRF family. (b) Conserved domains of *EgGRF* family members in oil palm. (c) Phylogenetic tree of the GIF family. (d) Conserved domains of *EgGIF* family members in oil palm.

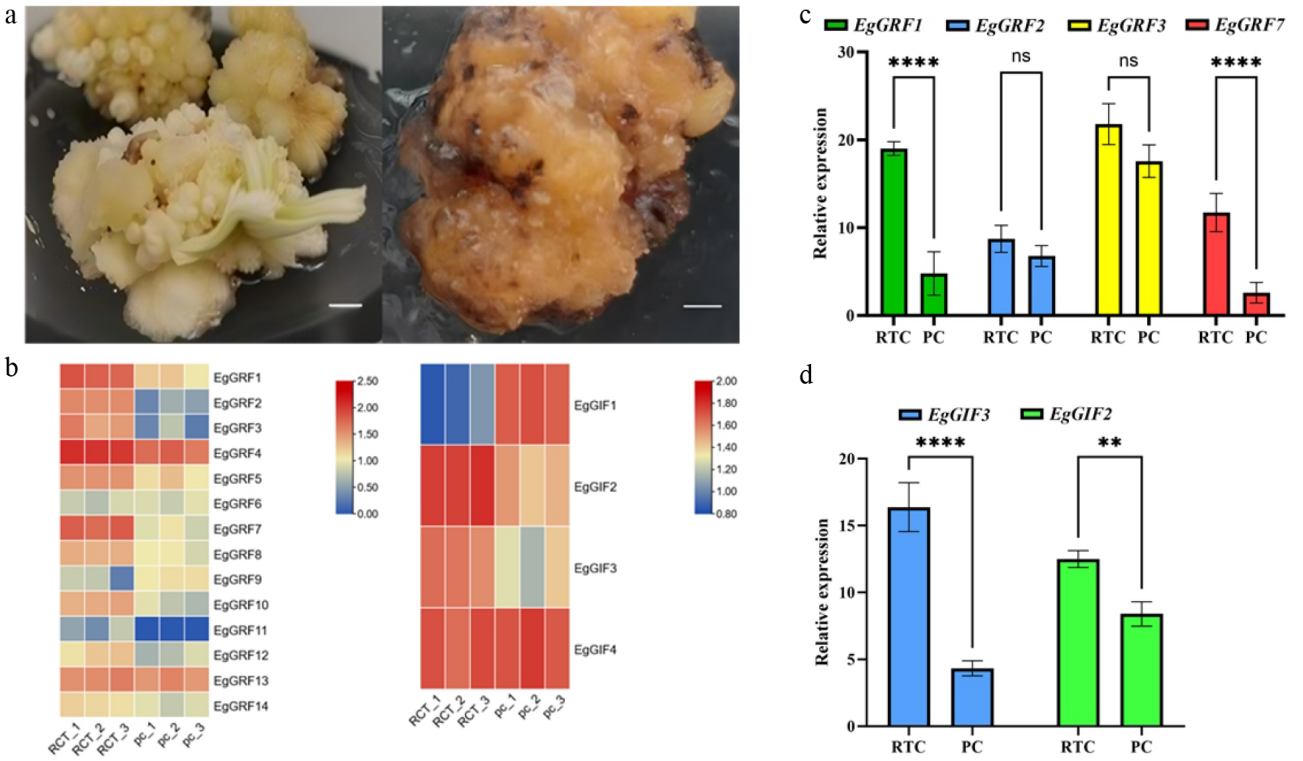

Fig. 2 Differential expression of *EgGRF* and *EgGIF* genes between robust regenerable callus (RC) and poorly growing callus (PC). (a) Oil palm callus at different physiological states. Scale bar = 5 mm. (b) Differential expression of oil palm *EgGIF* and *EgGRF* genes in callus tissue. (c) Differential expression of GRF genes in oil palm callus. (d) Differential expression of GIF genes in oil palm callus.

(Fig. 2c). In contrast, no significant differences were observed for *EgGRF*2 and *EgGRF*3 between the two callus types. Among the GIF genes, *EgGIF*3 showed highly significant upregulation in RC ($p < 0.0001$), whereas *EgGIF*2 showed a significant difference (Fig. 2d). These results suggest that *EgGRF*1, *EgGRF*7, and *EgGIF*3 may play important roles in oil palm callus proliferation and regeneration.

Protein–protein interaction between *EgGRF*1/*EgGRF7* and *EgGIF*3

To investigate whether *EgGRF*1 and *EgGRF7* physically interact with *EgGIF*3, a dual-luciferase complementation assay (LCI) was performed in *N. benthamiana* leaves (Fig. 3a, b). Strong luciferase activity was detected when nLUC-*EgGRF*1 was co-infiltrated with cLUC-*EgGIF*3 (Fig. 3c). Similarly, co-infiltration of nLUC-*EgGRF7* with cLUC-*EgGIF*3 also produced detectable luminescence (Fig. 3d). In contrast, no luciferase activity was observed in the negative control combinations (empty vectors or single constructs). These results demonstrate that both *EgGRF*1 and *EgGRF7* can physically interact with *EgGIF*3 in plant cells, providing a molecular basis for their potential synergistic function.

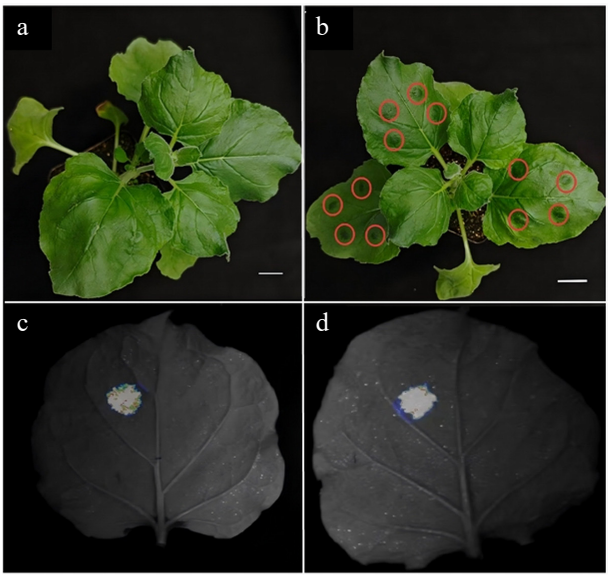

Fig. 3 Protein–protein interaction between *EgGRF*1/*EgGRF7* and *EgGIF*3 verified by LCI assay in *N. benthamiana* leaves. (a) Tobacco leaf before injection. (b) Tobacco leaf after injection. (c) Verification of dual-luciferase complementation of *EgGRF*1 and *EgGIF*3 genes in tobacco leaves. (d) Verification of dual-luciferase complementation of *EgGRF7* and *EgGIF*3 genes in tobacco leaves. Red circles indicate the injection sites. Scale bar = 1 cm.

Optimization of *Agrobacterium*-mediated transformation parameters

To improve the genetic transformation efficiency of oil palm callus, we systematically evaluated four key parameters: *Agrobacterium* concentration (OD_{600}), infection duration, acetosyringone (AS) concentration, and co-cultivation time. A factorial experiment with five OD_{600} values (0.4, 0.5, 0.6, 0.7, 0.8) and four infection durations (20, 30, 40, 50 min) was conducted. GFP-positive calli were observed in 12 out of 20 treatment combinations (Table 1). The highest screening efficiencies were achieved at OD_{600} = 0.6 with 30 min infection (3.32% ± 0.59%) and at OD_{600} = 0.5 with 40 min infection (3.45% ± 2.84%). Lower efficiencies (1.12%–2.26%) were observed in other treatments. Notably, no GFP-positive calli were obtained at the highest bacterial concentration (OD_{600} = 0.8) or the longest infection time (50 min) when combined with certain

https://doi.org/10.48130/tp-0026-0032

Table 1. Effects of *Agrobacterium* concentration and infection time on screening efficiency.

Level	Factors			
	OD_{600}	Time (min)	Number	GFP (%)
1	0.4	40	184	1.12 ± 1.05bc
2	0.6	50	176	0.00 ± 0.00c
3	0.8	50	144	0.00 ± 0.00c
4	0.6	20	167	1.82 ± 0.69bc
5	0.7	20	170	1.17 ± 1.23bc
6	0.5	20	187	0.00 ± 0.00c
7	0.6	30	178	3.32 ± 0.59ab
8	0.4	30	182	2.06 ± 2.01ab
9	0.4	20	163	0.00 ± 0.00c
10	0.7	30	166	0.00 ± 0.00c
11	0.6	40	166	2.21 ± 0.99ab
12	0.7	40	175	0.00 ± 0.00c
13	0.8	20	180	1.51 ± 1.44bc
14	0.8	30	158	1.47 ± 0.57bc
15	0.8	40	159	0.00 ± 0.00c
16	0.5	30	163	1.82 ± 3.15bc
17	0.7	50	169	0.00 ± 0.00c
18	0.5	50	160	1.95 ± 1.99ab
19	0.5	40	174	3.45 ± 2.84ab
20	0.4	50	173	2.26 ± 0.35ab

Different letters after the numbers (a, b, c) represent statistical differences between groups; values represent mean ± SD (n = 3).

OD_{600} values, likely due to callus browning and overgrowth of *Agrobacterium*.

AS concentrations ranging from 50 to 250 μmol/L were tested under optimal infection conditions (OD_{600} = 0.5, 40 min). The screening efficiency increased with AS concentration up to 200 μmol/L, reaching a maximum of 3.43%, and then declined at 250 μmol/L. Thus, 200 μmol/L AS was selected as the optimal concentration. Co-cultivation durations from 36 to 84 h were evaluated. The screening efficiency increased progressively from 36 to 60 h, peaking at 3.58% at 60 h, and then decreased at longer durations (Fig. 4a, b). Therefore, 60 h was determined as the optimal co-cultivation time. Under the optimized conditions (OD_{600} = 0.5, infection for 40 min, 200 μmol/L AS, 60 h co-cultivation), the average screening efficiency reached 3.58%. PCR confirmation using hygromycin-specific primers confirmed the presence of the transgene in hygromycin-resistant calli, while no band was detected in wild-type controls (Supplementary Fig. S2).

Effects of *EgGRF* and *EgGIF* overexpression on screening efficiency

To evaluate the functional roles of *EgGRF*1, *EgGRF*7, *EgGIF*3, and their co-expression in genetic transformation, we constructed single-gene overexpression vectors (35S:*EgGRF*1, 35S:*EgGRF*7, 35S:*EgGIF*3) and co-expression vectors (35S:*EgGRF*1-*EgGIF*3 and 35S:*EgGRF*7-*EgGIF*3). These constructs were introduced into oil palm callus using the optimized transformation protocol. After three to four rounds of selection on hygromycin-containing medium (9–12 weeks), transgenic materials at various developmental stages—including embryogenic calli, embryoids, and regenerated shoots—were harvested for molecular analysis. GFP fluorescence was detected in transgenic materials from all transformation treatments at different differentiation stages (Fig. 5a–f), whereas no fluorescence was observed in wild-type controls. PCR analysis was performed on genomic DNA extracted from hygromycin-resistant embryoids, which were the most abundant tissue type obtained after three to four rounds of selection. As shown in Supplementary Fig. S2, the hygromycin resistance gene was successfully amplified from transgenic embryoids across all construct types, while no amplification was detected in wild-type controls.

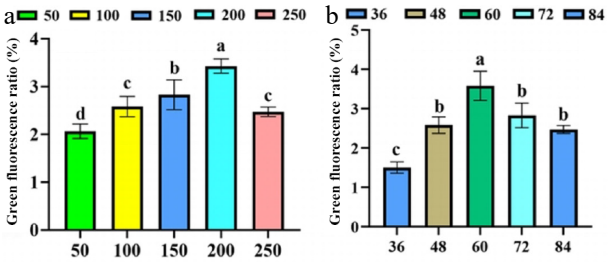

Fig. 4 Effects of (a) acetosyringone (AS) concentration, and (b) co-cultivation duration on *Agrobacterium*-mediated transformation efficiency of oil palm callus.

RT-qPCR analysis was performed on RNA extracted from transgenic embryoids, which provided the most consistent and abundant material for gene expression analysis. The results revealed that all transgenic embryoids exhibited significantly higher expression levels of the respective target genes compared to wild-type controls. Notably, the *EgGRF*1-*EgGIF*3 co-expression calli showed the highest expression levels among all transgenic lines (> 10-fold relative to WT), while *EgGRF*7-*EgGIF*3 co-expression calli exhibited even higher expression (> 15-fold). Single-gene transformants showed moderate but significant increases in target gene expression (Fig. 6a–c). The screening efficiency (GFP-positive rate) was calculated for each construct based on the number of GFP-positive embryoids obtained after three to four rounds of selection, as embryoids were the predominant differentiated structures at this stage. The *EgGRF*1-*EgGIF*3 co-expression group achieved the highest screening efficiency at 5.32% ± 0.34%, followed by *EgGRF*1 alone (4.35% ± 0.47%) (Fig. 7a). *EgGRF*7-*EgGIF*3 co-expression yielded an efficiency of 4.06% ± 0.22%, while *EgGRF*7 alone gave 3.46% ± 0.18%. *EgGIF*3 alone showed the lowest efficiency (2.48% ± 0.50%), which was not significantly different from the empty vector control. Statistical analysis indicated that *EgGRF*1-*EgGIF*3 co-expression significantly outperformed all other treatments ($p < 0.05$), while *EgGRF*1 alone also showed a significant improvement over the control.

Effects of *EgGRF* and *EgGIF* overexpression on callus differentiation

The differentiation capacity of transgenic materials was evaluated after three months of culture on selection medium. The materials scored for differentiation were regenerated shoots that had developed from embryoids (Supplementary Fig. S3), representing a more advanced developmental stage. Representative images showed that newly formed calli were cream-white in color and emerged from the surface of browned original calli. Notably, albino shoots were observed in some transgenic lines, particularly those transformed with *EgGRF*1, *EgGRF*1-*EgGIF*3, and *EgGRF*7-*EgGIF*3. After an additional three months under light culture conditions, distinct differentiation phenotypes were observed. Calli transformed with the empty vector, *EgGRF*7 alone, or *EgGIF*3 alone produced a small number of large shoots with low density. In contrast, *EgGRF*1-transformed calli produced multiple clustered shoots with dense, small leaves. The *EgGRF*1-*EgGIF*3 co-expression lines exhibited the most vigorous differentiation phenotype, with abundant clustered shoots and well-developed leaves. *EgGRF*7-*EgGIF*3 co-expression also promoted differentiation, producing shoots with complete leaves, though to a lesser extent than *EgGRF*1-*EgGIF*3 (Supplementary Fig. S3).

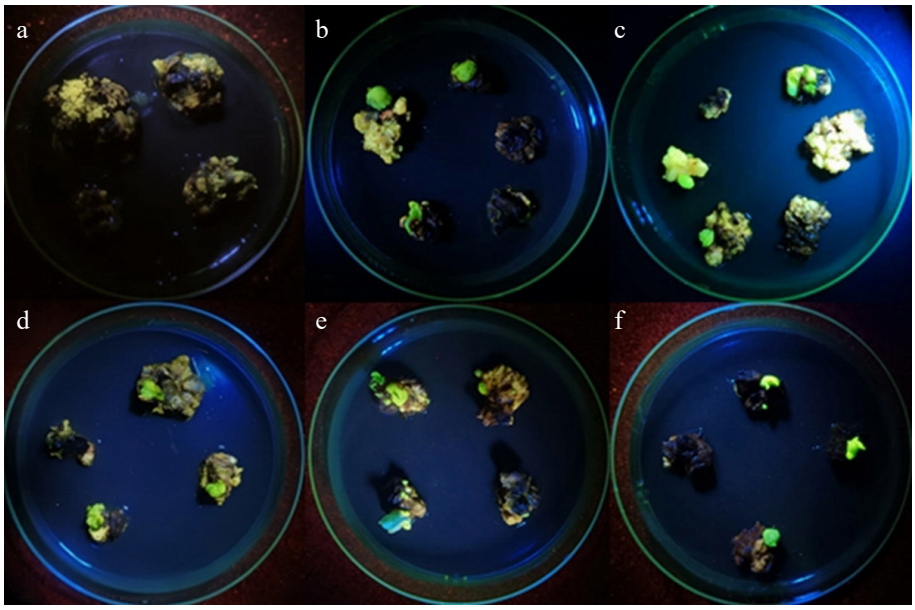

Fig. 5 Visualization and molecular confirmation of transgenic tissues. (a) Wild-type (CK). (b) *EgGRF*1. (c) *EgGRF*7. (d) *EgGIF*3. (e) *EgGRF*1-GIF3. (f) *EgGRF*7-GIF3.

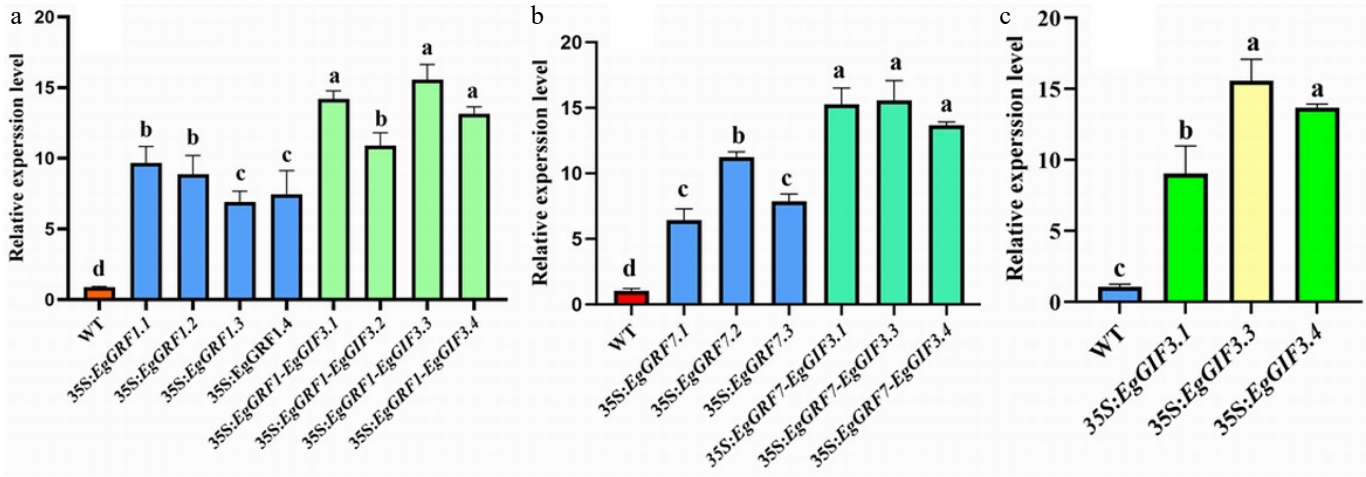

Fig. 6 Relative expression levels of target genes in transgenic embryoids. RT-qPCR analysis was performed on RNA extracted from transgenic embryoids obtained after three to four rounds of selection. (a) Expression levels in embryoids transformed with *EgGRF*7 and *EgGRF*1-*EgGIF*3. (b) Expression levels in embryoids transformed with *EgGRF*7 and *EgGRF*7-*EgGIF*3. (c) Expression levels in embryoids transformed with *EgGIF*3. Values are mean ± SD (n = 3). Different letters indicate significant differences ($p < 0.05$).

Quantitative analysis showed that the differentiation rate of the empty vector control was 19.27%. *EgGRF*1-*EgGIF*3 co-expression resulted in the highest differentiation rate (56.39%), followed by *EgGRF*1 alone (49.46%), with no significant difference between these two groups. *EgGRF*7-*EgGIF*3 co-expression gave a differentiation rate of 43.19%, while *EgGRF*7 alone reached 36.34%. *EgGIF*3 alone (22.69%) showed no significant improvement over the control (Fig. 7b). These results demonstrate that *EgGRF*1 plays a key positive role in oil palm callus differentiation, and its synergistic expression with *EgGIF*3 further enhances differentiation capacity at the embryogenic stage.

Discussion

In this study, 14 *EgGRF* and four *EgGIF* genes were identified in the oil palm genome, and we showed that *EgGRF*1, *EgGRF*7, and *EgGIF*3 were significantly upregulated in regenerable callus. Dual-luciferase assays confirmed physical interactions between *EgGRF*1/*EgGRF*7 and *EgGIF*3. We then optimized an *Agrobacterium*-mediated transformation protocol for oil palm embryogenic callus, achieving a screening efficiency of 3.58% under optimal conditions (OD_{600} = 0.5, infection for 40 min, 200 μmol/L AS, 60 h co-cultivation). Finally, we demonstrated that *EgGRF*1-*EgGIF*3 co-expression significantly increased both screening efficiency (5.32%) and differentiation rate (56.39%), outperforming single-gene transformations. These results establish *EgGRF*1 as a key positive regulator of oil palm callus differentiation and provide an effective strategy for improving genetic transformation screening and differentiation at the embryogenic stage in this recalcitrant species.

The number of GRF and GIF genes identified in oil palm (14 *EgGRF*s, four *EgGIF*s) is comparable to those in Arabidopsis (nine GRFs, three GIFs), rice (12 GRFs, three GIFs), and maize (15 GRFs, four GIFs), indicating that these gene families are highly conserved

https://doi.org/10.48130/tp-0026-0032

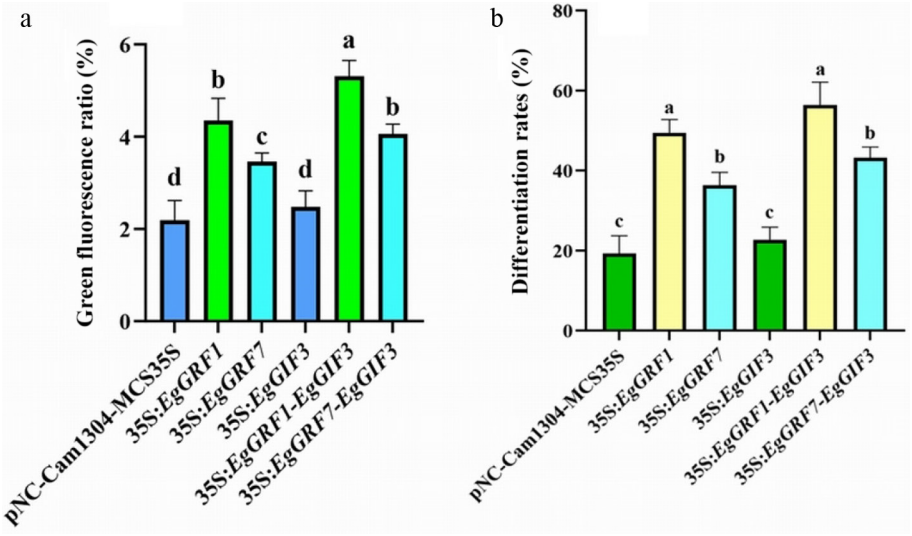

Fig. 7 Effects of *EgGRF* and *EgGIF* overexpression on screening efficiency and differentiation. (a) Screening efficiency based on GFP-positive embryoids after three to four rounds of selection. (b) Differentiation rate of transgenic regenerated shoots derived from embryoids. Values are mean ± SD (n = 3). Different letters indicate significant differences ($p < 0.05$).

across angiosperms[12,13,15]. The presence of conserved QLQ/WRC domains in all *EgGRF* proteins and SSXT domains in all *EgGIF* proteins further supports functional conservation of the GRF-GIF regulatory module. Our optimized transformation protocol (3.58% screening efficiency) represents a notable improvement over previously reported efficiencies in oil palm, which typically ranged from 0.7% to 2.0%[9,10]. The optimal AS concentration (200 μmol/L) and co-cultivation time (60 h) identified in our study are consistent with protocols for other recalcitrant monocots, which often require stronger Vir gene induction and longer co-cultivation periods compared to herbaceous plants[11]. The finding that *EgGRF*1-*EgGIF*3 co-expression enhances screening efficiency and differentiation capacity aligns with the landmark study by Debernardi et al.[22], who showed that GRF-GIF chimeric proteins improve transformation and regeneration efficiency in wheat, rice, and citrus. Notably, while Debernardi et al. demonstrated whole-plant regeneration, our study focuses on the callus/embryogenic stage as a platform for rapid functional gene validation in oil palm. Notably, *EgGRF*1 alone significantly improved differentiation rate (49.46%), whereas *EgGIF*3 alone showed no effect, consistent with the role of GIFs as co-activators that require GRF partners to function[19].

Taken together, to our knowledge, this is the first comprehensive analysis of GRF and GIF genes in oil palm and demonstrates the practical application of GRF-GIF co-expression to enhance genetic transformation in this crop. PCR and GFP analyses confirmed transgene integration and expression in transgenic materials at multiple stages of *in vitro* development, including embryogenic calli, embryoids, and regenerated shoots. These data demonstrate that the *EgGRF*1-*EgGIF*3 co-expression module promotes not only screening efficiency at the callus stage but also differentiation capacity leading to early shoot formation. However, it should be clearly stated that the production of complete, soil-grown transgenic plants was not pursued in this study, as the primary objective was to establish an efficient transformation platform at the callus/embryogenic stage for rapid functional gene validation in oil palm—a species in which stable transformation and regeneration remain notoriously time-consuming (typically requiring approximately 1 year from callus to plantlet). Whether the improved efficiencies observed at the callus/embryogenic stage translate to full plant regeneration remains an important question for future investigation.

Ethical statements

During the preparation of this work, the authors used ChatGPT (GPT-5.5, OpenAI; Date of Use: August 2026) and the OpenAI Image Generation tool to assist in the conceptual design and preparation of the Graphical Abstract. The AI tools were used solely to generate an initial conceptual illustration based on the authors' original research. The authors reviewed, revised, and manually edited the AI-generated content to ensure its scientific accuracy and consistency with the manuscript. The authors take full responsibility for the integrity, originality, and accuracy of the final manuscript and figures. No AI tool is credited as an author.

Author contributions

The authors confirm their contributions to the paper as follows: supervision, resources, funding acquisition: Zou J, Li D; data collection: Luo C, Zhang T, Yuan F; analysis and interpretation of results: Luo C, Ouyang C, Zou J; draft manuscript preparation: Luo C, Li D. All authors reviewed the results and approved the final version of the manuscript.

Data availability

The datasets generated during and/or analyzed during the current study are not publicly available because they are being used in ongoing research but are available from the corresponding author on reasonable request.

Acknowledgments

This research was supported by the National Natural Science Foundation of China (NSFC) (U23A20220 and 32260064) and the China Agriculture Research System (CARS-14).

Conflict of interest

The authors declare that they have no conflict of interest.

Supplementary information accompanies this paper online at: https://doi.org/10.48130/tp-0026-0032.

Dates

Received 20 April 2026; Revised 14 July 2026; Accepted 22 July 2026; Published online 18 September 2026

References

[1] Murphy DJ. 2025. Agronomy and environmental sustainability of the four major global vegetable oil crops: oil palm, soybean, rapeseed, and sunflower. *Agronomy* 15:1465

[2] Corley RHV, Tinker PB. 2016. *The Oil Palm*. 5th Edition. Chichester, England: Wiley Blackwell. 688 pp. doi: 10.1002/9781118953297

[3] Cao HX, Yang YD, Shi P, Lei XT. 2016. A retrospect and prospect of research on the evaluationof oil palm germplasm resources. *Chinese Journal of Tropical Agricultural Science* 36:59–62 (in Chinese)

[4] Weckx S, Inzé D, Maene L. 2019. Tissue culture of oil palm: finding the balance between mass propagation and somaclonal variation. *Frontiers in Plant Science* 10:722

[5] Abdullah R, Zainal A, Heng WY, Li LC, Beng YC, et al. 2005. Immature embryo: a useful tool for oil palm (*Elaeis guineensis* Jacq.) genetic transformation studies. *Electronic Journal of Biotechnology* 8:24–34

[6] Low ETL, Alias H, Boon SH, Shariff EM, Tan CYA, et al. 2008. Oil palm (*Elaeis guineensis* Jacq.) tissue culture ESTs: identifying genes associated with callogenesis and embryogenesis. *BMC Plant Biology* 8:62

[7] Ahmad Parveez GK, Rasid OA, Masani MYA, Sambanthamurthi R. 2015. Biotechnology of oil palm: strategies towards manipulation of lipid content and composition. *Plant Cell Reports* 34:533–543

[8] Chilton MD, Drummond MH, Merlo DJ, Sciaky D, Montoya AL, et al. 1977. Stable incorporation of plasmid DNA into higher plant cells: the molecular basis of crown gall tumorigenesis. *Cell* 11:263–271

[9] Izawati AMD, Masani MYA, Ismanizan I, Ahmad Parveez GK. 2015. Evaluation on the effectiveness of 2-deoxyglucose-6-phosphate phosphatase (*DOG^{R}1*) gene as a selectable marker for oil palm (*Elaeis guineensis* Jacq.) embryogenic calli transformation mediated by *Agrobacterium tumefaciens*. *Frontiers in Plant Science* 6:727

[10] Hanin AN, Masani MYA, Janna OA, Rasid OA, Ahmad Parveez GK. 2025. *Agrobacterium*-mediated genome modification for improvement of oil palm planting materials. *OBM Genetics* 9:292

[11] Chen Z, Liao WH, Wang JC, Gao K, Sun J, et al. 2014. Factors affecting *Agrobacterium*-mediated genetic transformation of poplar. *Plant Physiology Journal* 50:1126–1134 (in Chinese)

[12] Kim JH, Choi D, Kende H. 2003. The *AtGRF* family of putative transcription factors is involved in leaf and cotyledon growth in *Arabidopsis*. *The Plant Journal* 36:94–104

[13] Choi D, Kim JH, Kende H. 2004. Whole genome analysis of the *OsGRF* gene family encoding plant-specific putative transcription activators in rice (*Oryza sativa* L.). *Plant & Cell Physiology* 45:897–904

[14] Chen F, Yang Y, Luo X, Zhou W, Dai Y, et al. 2019. Genome-wide identification of GRF transcription factors in soybean and expression analysis of *GmGRF* family under shade stress. *BMC Plant Biology* 19:269

[15] Cui JH, Yang PY, Chang JH. 2021. Identification and expression analysis under abiotic stress of *GRF* gene family in sorghum. *Journal of Agricultural Science and Technology* 23:37–46 (in Chinese)

[16] Sun ZT, Wang XY, Hou LL, Liu YY, Zheng ZM. 2025. Identification and preliminary functional analysis of *BpGRFs* genes in *Betula platyphylla*. *Bulletin of Botanical Research* 45:191–201 (in Chinese)

[17] Perani M, Ingram CJE, Cooper CS, Garrett, MD, Goodwin GH. 2003. Conserved SNH domain of the proto-oncoprotein SYT interacts with components of the human chromatin remodelling complexes, while the QPGY repeat domain forms homo-oligomers. *Oncogene* 22:8156–8167

[18] Lee BH, Ko JH, Lee S, Lee Y, Pak JH, et al. 2009. The Arabidopsis *GRF-INTERACTING FACTOR* gene family performs an overlapping function in determining organ size as well as multiple developmental properties. *Plant Physiology* 151:655–668

[19] Kim JH. 2019. Biological roles and an evolutionary sketch of the GRF-GIF transcriptional complex in plants. *BMB Reports* 52:227–238

[20] Wang F, Qiu N, Ding Q, Li J, Zhang Y, et al. 2014. Genome-wide identification and analysis of the growth-regulating factor family in Chinese cabbage (*Brassica rapa* L. ssp. pekinensis). *BMC Genomics* 15:807

[21] Zhang B, Tong Y, Luo K, Zhai Z, Liu X, et al. 2021. Identification of GROWTH-REGULATING FACTOR transcription factors in lettuce (*Lactuca sativa*) genome and functional analysis of *LsaGRF5* in leaf size regulation. *BMC Plant Biology* 21:485

[22] Debernardi JM, Tricoli DM, Ercoli MF, Hayta S, Ronald P, et al. 2020. A GRF–GIF chimeric protein improves the regeneration efficiency of transgenic plants. *Nature Biotechnology* 38:1274–1279

Copyright: © 2026 by the author(s). Published by Maximum Academic Press on behalf of Hainan University. This article is an open access article distributed under Creative Commons Attribution License (CC BY 4.0), visit https://creativecommons.org/licenses/by/4.0/.